

1 Article

# 2 CRISP-R/Cas9 Mediated Deletion of Copper 3 Transport Genes CTR1 and DMT1 in NSCLC Cell 4 Line H1299. Biological and pharmacological 5 consequences

6 Ekaterina Y. Ilyechova <sup>1,2,3</sup> Elisa Bonaldi <sup>4</sup>, Iurii A. Orlov <sup>1</sup>, Ekaterina Skomorokhova <sup>1</sup>, Ludmila V.  
7 Puchkova <sup>1,2,3\*</sup>, Massimo Brogginì <sup>1,4</sup>

8 <sup>1</sup>→Laboratory of Trace elements metabolism, ITMO University, Kronverksky av., 49, St.-Petersburg 197101,  
9 Russia; e.boglaeva@corp.ifmo.ru

10 <sup>2</sup> Department of Molecular Genetics, Research Institute of Experimental Medicine, Acad. Pavlov str., 12,  
11 St.-Petersburg 197376, Russia; iem@iemrams.ru

12 <sup>3</sup> Department of Biophysics, Peter the Great St. Petersburg Polytechnic University, Politekhnikeskaya str.,  
13 29, St.-Petersburg 195251 Russia; odo@spbstu.ru

14 <sup>4</sup>→Laboratory of molecular pharmacology, Istituto di Ricerche Farmacologiche “Mario Negri” IRCCS, Via La  
15 Masa, 19, 20156 Milan, Italy;

16 \* Correspondence: puchkova@yandex.ru; Tel.: +7-821-234-33-56

17

18 **Abstract:** Copper, the highly toxicity micronutrient, plays two essential roles: it is a catalytic and  
19 structural cofactor for Cu-dependent enzymes, and it acts as a secondary messenger. In the cells,  
20 copper is imported by CTR1, a transmembrane high-affinity copper importer, and DMT1 (divalent  
21 metal transporter). In cytosol, enzyme-specific chaperones receive copper from CTR1 C-terminus  
22 and deliver it to their apoenzymes. DMT1 cannot be a donor of catalytic copper because it does not  
23 have cytosol domain which is required for copper transfer to the Cu-chaperons and following to  
24 cuproenzymes. Here we assume that DMT1 can mediate copper way required for regulatory  
25 copper pool. To verify this thought, we used CRISPR/Cas9 to generate H1299 cell line with CTR1 or  
26 DMT1 single knockout (KO) and CTR1/DMT1 double knockout (DKO). To confirm KOs of the  
27 genes qRT-PCR were used. Two independent clones for each gene were selected for further studies.  
28 In CTR1-KO cells, expression of the DMT1 gene was significantly increased. In subcellular  
29 compartments, copper concentration decreased dramatically in DKO cells. CTR1-KO cells, but not  
30 DMT1-KO, demonstrated reduced sensitivity to cisplatin and silver ions, agents that enter the cell  
31 through CTR1. The expression of genes, whose protein products require copper: HIF1 $\alpha$ , XIAP,  
32 COMMD1, CCS, Cp, but not SOD1 and NF-kB, changed their level. Perhaps these data will help to  
33 understand how the disturbances of copper homeodynamics lead to the development of  
34 neurodegenerative and oncological disorders. Possibility of using CTR1 KO and DMT1 KO cells to  
35 study homeodynamics of catalytic and signaling copper selectively is discussed.

36 **Keywords:** copper importers CTR1 and DMT1, CRICPR-Cas9, cisplatin, silver, signaling, copper  
37 homeodynamics

38

## 39 1. Introduction

40 In mammals, copper has two essential physiological functions. First, it is a catalytic and  
41 structural cofactor of enzymes necessary for respiration, antioxidant protection, post-translational  
42 modification of neuropeptides, for the synthesis of neurotransmitters, for the formation of collagen  
43 and elastin, for iron transport, etc. [1,2]. Second, copper inside and outside the cell is required for  
44 the activity of some regulatory proteins (HIF1 $\alpha$ , XIAP, COMMD1, NF-kB, p53), which are involved in  
45 signaling pathways [3-7]. The indispensable biological functions of copper are inseparable from its

46 high toxicity, which is compensated by an intricately system of carriers that coordinate copper  
47 through specific sites, and safely transfer it from the extracellular space to the cell places of  
48 cuproenzyme formation (mitochondria, Golgi apparatus, cytosol) [8].

49 It is still unclear how copper is recruited into signaling pathways, or how it is secreted from the  
50 cell to participate in neovascularization [9]. As a non-sophisticated version of this issue, it can be  
51 assumed that these copper streams enter the cell through different gates. The main universal  
52 importer of copper in mammalian cells is CTR1 [10,11]. It is a transmembrane homotrimer, each  
53 subunit of which contains 3  $\alpha$ -helices, forming a transmembrane domain of 9  $\alpha$ -helices. The  
54 N-terminal extracellular domain contains 3 Cu(II)/Cu(I) sites. In a homotrimer, N-termini form a  
55 high affinity copper trap from the environment, where its concentration is low. The short C-terminal  
56 domain contains a copper-binding HCH-motif. All cytosolic copper carriers required for  
57 cuproenzymes, taking delivered copper, due to a protein-protein interaction with C-domain CTR1  
58 [12]. One might think that catalytic copper enters through the CTR1.

59 The cells contain another importer, also capable of carrying copper. It is the divalent metal  
60 transporter 1 (DMT1), also known as divalent cation transporter 1 (DCT1) and natural  
61 resistance-associated macrophage protein 2 (NRAMP 2), the member 2 of solute carrier family [13].  
62 It consists of a single subunit. Putative topological DMT1 model predicts that DMT1 is a type III  
63 integral membrane protein (both N- and C-terminus are oriented to the cytoplasm), with  
64 transmembrane domain from 12  $\alpha$ -helices and two sites for core N-glycosylation in the extracellular  
65 loop between 7 and 8  $\alpha$ -helices [14]. It's well established that it functions as proton-coupled pump  
66 by using the cell membrane potential for active transport. DMT1 imports iron as Fe(II), and also  
67 Mn(II), Zn(II), Cu(II), Ni(II), Co(II), Pb(II) and Cd(II) ions; it is ubiquitously expressed, most notably  
68 in the apical membrane of the enterocytes in duodenum [13]. The cation binding peptide is formed  
69 by DMT1- $\alpha$ -helix1 as an  $\alpha$ -helix-extended segment- $\alpha$ -helix configuration, in which the negative  
70 charged motif Asp-Pro-Gly-Asn responsible for cation binding is located at the central flexible  
71 region [15].

72 DMT1 transports copper in both Cu(II)/Cu(I) oxidation states [16], and even when the CTR1  
73 gene is switched off, it compensates for its deficiency [17]. C-terminal domain of DMT1 has no  
74 homology with C-terminus of CTR1, so, it is unlikely that it is capable of transferring copper to  
75 cuproenzyme-associated Cu-transporters. It is yet not known which proteins, or low molecular  
76 weight substances, take copper from DMT1. It is possible that DMT1 represents the pathway for  
77 regulatory copper. To check this hypothesis, we obtained single knockout CTR1 and DMT1 cells as  
78 well as double knockout of both genes. Engineered cells were tested for resistance to cisplatin and  
79 silver ions, and to some additional drugs acting with different mechanisms of action. The expression  
80 profile of genes coding copper-requiring proteins was also determined.

## 81 2. Materials and Methods

### 82 2.1. Cell lines

83 The human non small cell lung cancer cell line H1299 was used for these experiments. These  
84 cells do not express the tumor suppressor p53 protein. Cells were grown in RPMI medium  
85 supplemented with 10% FBS. Cells were transfected with CRISPR-Cas9 KO plasmids with three  
86 targets specific guide RNAs (gRNA) of 20 nt (for both CTR1 and DMT1 genes). The plasmids were  
87 co-transfected with Homology-Directed Repair (HDR) plasmids specific for each gene (Santa Cruz  
88 Biotechnology), which allow the insertion of puromycin resistance gene and red fluorescent protein  
89 (RFP) gene during the repair process. Puromycin and RFP genes can then be removed using Cre  
90 recombinase, thanks to the presence of loxP sites in HDR plasmids.

91 Cells were seeded at high density 24 hours before transfection in 6 well plates. Fugene  
92 (promega) was used as transfection reagent. Twenty-four hours after transfection, cells were  
93 detached and seeded in 10 ml Petri dishes at a density of 500 cells /plate. After the following 48  
94 hours, puromycin (2  $\mu$ g/ml) was added to allow selection of positive clones. A double selection of  
95 clones growing in puromycin containing medium and expressing RFP was performed. Positive  
96 clones were isolated and transferred to 6 well plates.

97 Expression of CTR-1 or DMT-1 mRNA by RT-Real time PCR was used to confirm the KO of the  
98 genes. Two independent clones for each gene were selected for further studies.

99 For generation of double KO cells (for both CTR-1 and DMT-1 genes) one clone deleted in  
100 CTR-1 was treated with Cre recombinase to remove puromycin and RFP genes and subjected to a  
101 second round of transfection using a mix of DMT-1 KO plasmid and DMT-1 HDR plasmid using the  
102 same procedure as described for single KO generation.

#### 103 104 2.2. RT-Real Time PCR

105 Total RNA was extracted from exponentially growing cells using Maxwell RSC simply RNA  
106 Cells kit (Promega) and reverse-transcribed to cDNA using High Capacity cDNA Reverse  
107 Transcription Kit (Life Technologies). DMT1, CTR1, XIAP, HIF1 $\alpha$ , NF- $\kappa$ B, COMMD1, CCS, SOD1  
108 expression levels were determined by real time RT-PCR performed with Sybr Green PCR master mix  
109 (Applied Biosystem). For each gene and each sample, the dissociation curve was evaluated. Samples  
110 were then normalized using the expression of the housekeeping gene (actin) and the levels in the KO  
111 clones were compared to parental cells. Real-time PCR was performed using the 7900HT Sequence  
112 Detection System (Applied Biosystems).

#### 113 114 2.3. Cell growth and cytotoxicity

115 The growth in vitro of the different clones was determined using the RealTime GLO system  
116 (Promega). All the procedures were performed according to the manufacturing instructions.  
117 Luminescence was detected at 24 hours interval using the GloMax plate reader (Promega). For each  
118 clone 6 independent samples were assessed, and the mean doubling time calculated from the linear  
119 part of the growth curve for each cell line.

120 The growth inhibitory activity of two platinum containing drugs, cisplatin and carboplatin, of  
121 the mTOR inhibitor Torin-1, of the ATR inhibitor VE-822, of the GLUT-1 inhibitor STF-31 and of the  
122 widely used antidiabetic drug metformin, was determined in the different clones by using the MTS  
123 test. Cells were seeded in 96 wells plates and after 24 hours treated with increasing concentrations of  
124 the drugs for further 72 hours. Survival curves were plotted as percentages of untreated controls. At  
125 least 6 replicates for each time point were used and the results represent the average mean and SD of  
126 at least 3 independent experiments.

#### 127 128 2.4. Isolation of subcellular fractions

129 Subcellular fractions were isolated by differential centrifugation. Cells were homogenized (1:6  
130 w/v, respectively) in buffer A, containing 250 mM sucrose, 100 mM KCl, 5 mM MgCl<sub>2</sub>, 10 mM  
131 Tris-HCl (pH 7.4), 5 mM DTT, and 0.5  $\mu$ l/ml of protease inhibitor cocktail (Sigma, USA), using T10  
132 basic homogenizer for 3 $\times$ 20 s at maximum power (IKA, Germany). The homogenate was centrifuged  
133 at 800 $\times$ g for 10 min. A crude mitochondrial fraction was isolated from the post-nuclear supernatant  
134 as sediment after centrifugation at 12,000 $\times$ g for 20 min. A total intracellular membrane fraction  
135 (endoplasmic reticulum + Golgi complex) was isolated from the post-mitochondrial supernatant as  
136 sediment at 23,000 $\times$ g, 60 min. The supernatant of the last centrifugation comprised the cytosolic  
137 fraction.

138  
139 2.5. Expression of Cp secreted in the medium was assessed by immunoblotting (WB) in samples  
140 of cell culture supernatants. Twenty-five microliters of cultured medium were separated on 8%  
141 polyacrylamide gels (PAG) by nondenatured electrophoresis according to the Laemmli method.  
142 The protein transfer, control for the quality of transfer with Ponceau staining, blocking with 5%  
143 non-fat milk, blotting with primary antibodies, and visualization of the immune complexes were  
144 described previously [18]. Hybond ECL nitrocellulose membrane, ECL reagent, ECL Hyperfilm (GE  
145 Healthcare, USA), and horseradish peroxidase-conjugated goat anti-rabbit secondary antibodies  
146 (Abcam, UK) were used for the WB analysis. In the work, non-commercial antibodies to high purity  
147 human ceruloplasmin were used [19].  
148

149           2.6. *Preparation the growth medium saturated with silver ions*

150           The portions of AgCl crystals were added to RPMI medium with stirring until AgCl crystals  
151 ceased to dissolve. Ag-medium was clarified by centrifugation at 10000×g, 1 h. This medium was  
152 considered as saturated with Ag(I) growth medium, in which silver atoms are coordinated. Silver  
153 concentration in the Ag-saturated medium was determined by atomic absorption spectrometry. It  
154 was 150 μM.

155  
156           2.7. *Measurement of metal concentration*

157           Copper and silver concentrations were measured by graphite furnace atomic absorption  
158 spectrometry (FAAS) with electrothermal atomization and Zeeman correction of nonselective  
159 absorption on a ZeeNit P650 spectrometer (Analytik Jena, Germany) with automatic sampling  
160 duplication. The samples were dissolved in pure concentrated HNO<sub>3</sub>.

161  
162           2.8. *Statistical analysis*

163           The statistical analysis was performed using GraphpadPrism version 6.07. Differences between  
164 groups were considered statistically significant, when the p-values were ≤0.05.

165           **3. Results**

166           Using H1299 cells, we generated CTR1 and DMT1 single KO clones using CRISPR-Cas9 system.  
167 Two independent homozygous KO clones for each gene were selected (clone 45 and 46 for CTR1 and  
168 clones 20 and 31 for DMT1). From a CTR1 KO clone (clone 45) a second round of transfection,  
169 following excision of puromycin and RFP genes by Cre recombinase, to generate CTR1-/DMT1  
170 double KO. These last clones were less efficiently generated compared to single KO genes. In fact,  
171 while we could isolate several CTR1<sup>-/-</sup> or DMT1<sup>-/-</sup> clones, we were only able to isolate one CTR1<sup>-/-</sup>,  
172 DMT1<sup>+/-</sup> (DKO 4) clone and one CTR1<sup>-/-</sup>, DMT1<sup>-/-</sup> clone only (DKO 5). The majority of the  
173 experiments were performed in one CTR1<sup>-/-</sup> clone, one DMT1<sup>-/-</sup> clone and one DKO clone, and  
174 some results were confirmed in the second generated clone for each genotype.

175           Selected clones were initially tested for their ability to grow in vitro. Table 1 reports the  
176 doubling times (DT) calculated on three independent experiments, each consisting of six replicates.  
177 As it can be seen the selected clones have similar DT all growing slightly faster than parental H1299  
178 cells.

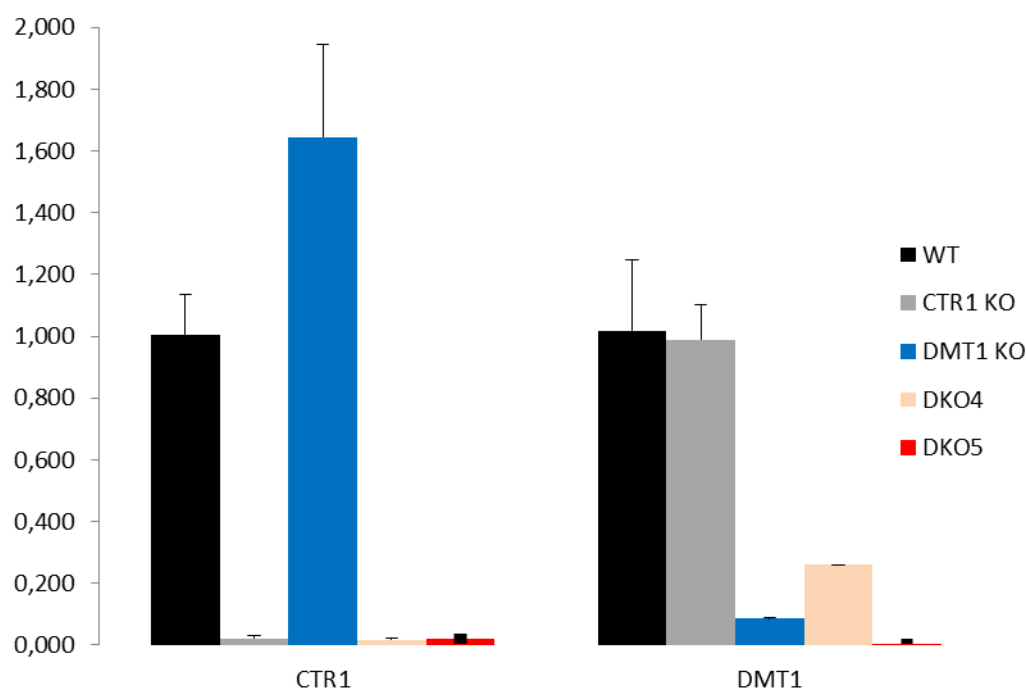
179

180           **Table 1.** Doubling time of H1299-derive clones

CELL LINE	DOUBLING TIME, (h) ±SD
H1299	18.77±1.49
CTR1 KO45	15.03±4.09
DMT1 KO31	13.45±2.31
DKO 4 (CTR1 <sup>-/-</sup> , DMT1 <sup>+/-</sup> )	14.51±3.30
DKO 5 (CTR1 <sup>-/-</sup> , DMT1 <sup>-/-</sup> )	15.36±2.56

181

182           Figure 1 displays the estimates of expression of DMT1 and CTR1 by RT-Real time PCR in  
183 parental H1299 cells, in one clone KO for CTR1 (clone 45), one clone KO for DMT1 (clone 31), one  
184 clone CTR1<sup>-/-</sup>, DMT1<sup>+/-</sup> (DKO 4), and one clone CTR1<sup>-/-</sup>, DMT1<sup>-/-</sup> (DKO 5).



185

186

187

**Figure 1.** RT-Real time PCR analysis of CTR1 and DMT1 mRNA expression in the different clones. Ordinate: concentration mRNA of CTR1 or DMT1 to actin-mRNA.

188

189

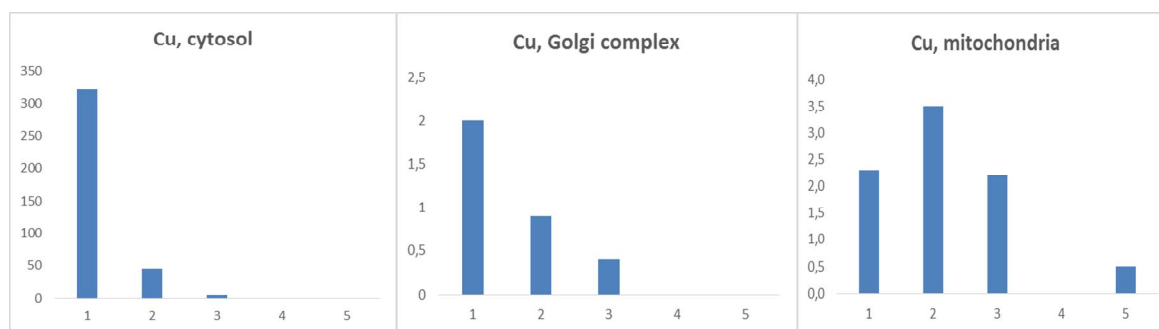
190

191

192

193

A clear lack of expression of the respective target genes is seen for single KO cells. DKO 5 clone showed a dual inhibition of expression, and DKO 4 clone, which is DMT1<sup>+/-</sup> heterozygous clone, expresses DMT1 2 times higher than DMT1<sup>-/-</sup>. Interestingly CTR1 KO clone showed a consistent increase in DMT1 expression, while in the DMT1 KO clone the expression of CTR1 was similar to that of parental cells.



194

195

196

**Figure 2.** Copper distribution in CTR1 KO, DMT1 KO and DKO cells. Ordinate: copper concentration (µg/L) in subcellular fractions. 1 – control, 2 – CTR1/45, 3 – DMT1/31, 4 – DKO5, 5 – DKO4.

197

198

199

200

201

202

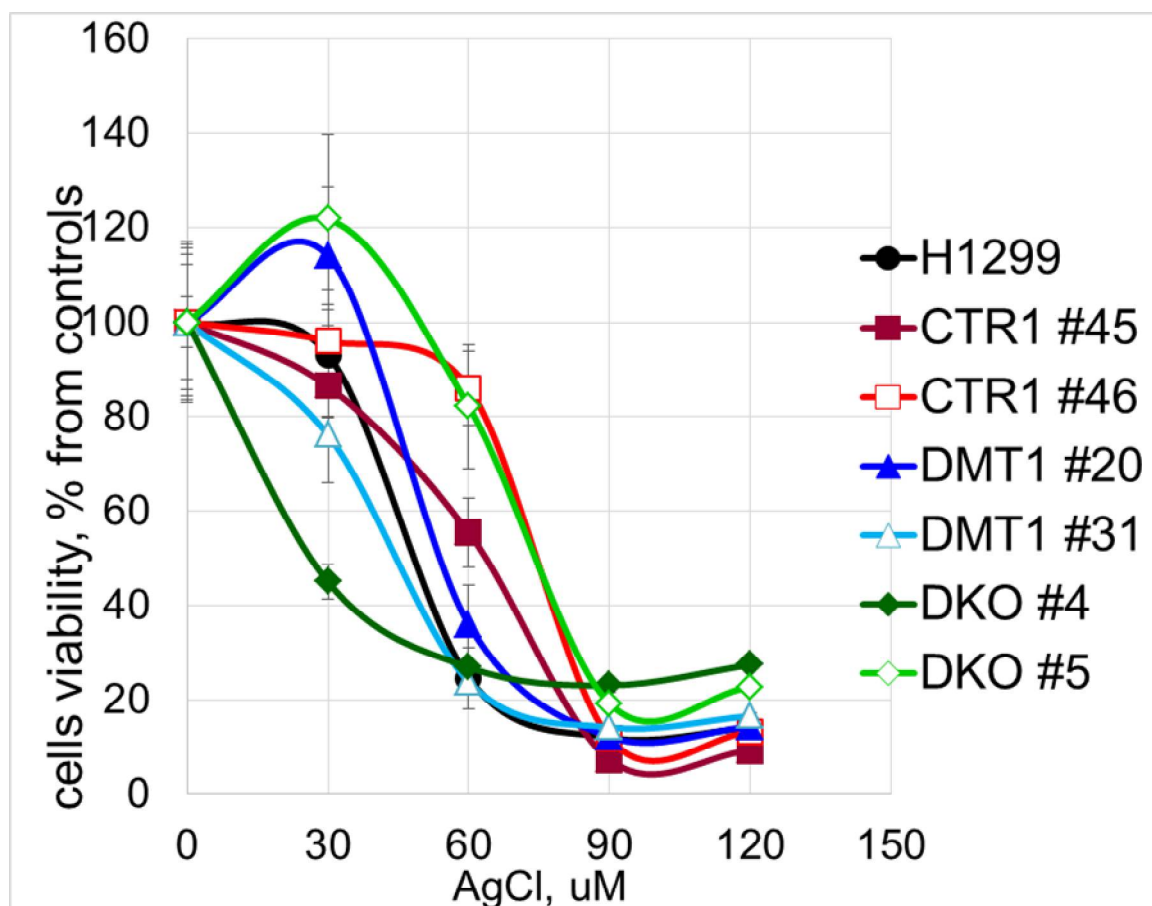
203

204

205

206

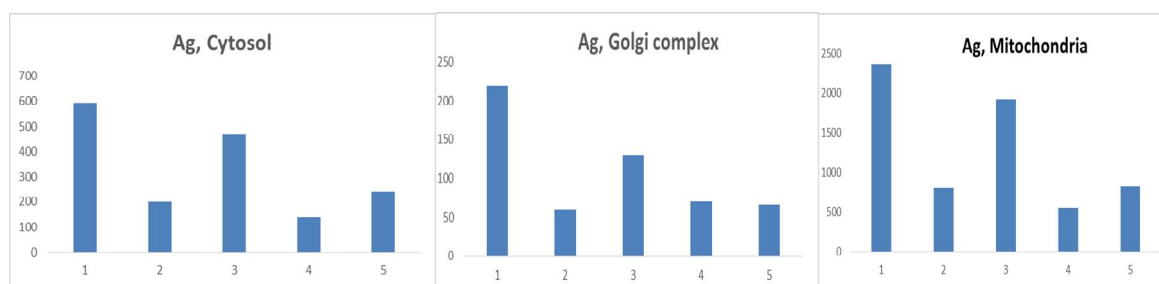
The effects of the single and double knockout of CTR1 and DMT1 on copper distribution in the cells are shown in Figure 2. In cytosol of CTR1 KO/45, the copper level decreased by a factor of 6. In DMT1 KO clone, the copper content was even lower, and in DKO, the content of copper dropped further below the threshold of reliable measurements. In the Golgi apparatus, the copper level in CTR1-KO/45 decreased almost twofold, in DMT1 KO/31, it was roughly 1/8 of that of parental cells while in the two DKO clones the levels of copper in Golgi were below the detection level. In the mitochondria of cells with single knockouts, the copper content remained almost unchanged, but it sharply decreased in both DKO cells. The cells were tested for the toxic effect of silver ions. Figure 3 demonstrates that CTR1-KO clones are more resistant to silver ions than wild-type (WT) cells, or DMT1-KO clones.



207  
208

**Figure 3.** Cells viability after treatment in medium with AgCl for 72 hours.

209 In these clones, the distribution of silver was traced at different concentrations in medium  
210 (Figure 4). In the cytosol, the Golgi complex membranes and in the mitochondria, in DMT1-KO  
211 clones, silver content was about the same as in WT cells. At the same time in CTR1-KO and DKO  
212 clones compartments, the silver concentration was 3 to 5 times lower.  
213

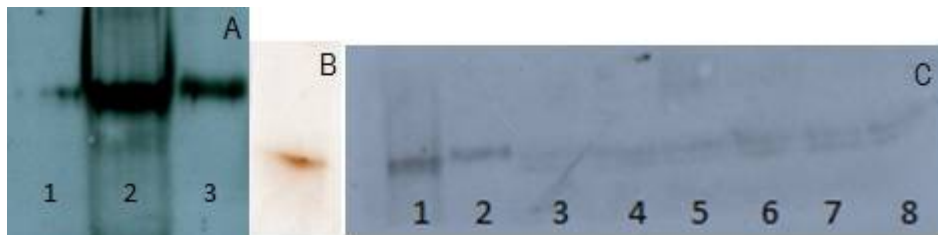


214  
215  
216

**Figure 4.** Silver distribution in CTR1 KO, DMT1 KO and DKO cells. Ordinate: silver concentration ( $\mu\text{g/L}$ ) in subcellular fractions. 1 – control, 2 – CTR1/45, 3 – DMT1/31, 4 – DKO5, 5 – DKO4.

217 Using the example of ceruloplasmin, we checked the ability of the obtained clones to synthesize  
218 secretory cuproenzymes. Ceruloplasmin, a polyfunctional blue (ferr)oxidase of hepatic origin, is the  
219 main copper-containing blood serum protein [20–22]. It has been shown that ceruloplasmin is also  
220 synthesized in the lungs [23], its function has not been established. We first checked whether fetal  
221 calf serum (FSB) will give false positive signals in WB analysis. The data in Figure 5A shows that FSB  
222 does not give a positive signal with antibodies to human ceruloplasmin. WT H1299 cells synthesize  
223 and secrete ceruloplasmin (Figure 5A), which by mobility corresponds to holo-ceruloplasmin. In  
224 CTR1-KO, DMT1-KO and DKO cells, the synthesis of immunoreactive ceruloplasmin decreased

225 (Figure 5C). Moreover, in all KO clones, ceruloplasmin was detected as two bands that correspond to  
 226 holo- and apo-ceruloplasmin [24].  
 227



228

229

230

231

232

233

**Figure 5.** Ceruloplasmin gene activity in CTR1-KO, DMT1 KO, and DKO. **(A)** WB of 8% non-denaturated PAGE, 1 – FSB, 0.5  $\mu$ l per line; 2 – human serum, 0.025  $\mu$ l per line; 3 – H1299 medium of cultivation, 25  $\mu$ l per line. **(B)** human serum, 0.025  $\mu$ l per line, gel was stained with orto-dianisidine; **(C)** 1 – human serum, 0.025  $\mu$ l per line; 2 – H1299, 3 – CTR1 45, 4 – CTR1 46, 5 – DMT1 31, 6 – DMT1 20, 7 – DKO 4, 8 – DKO 5, 25  $\mu$ l medium per line

234

235

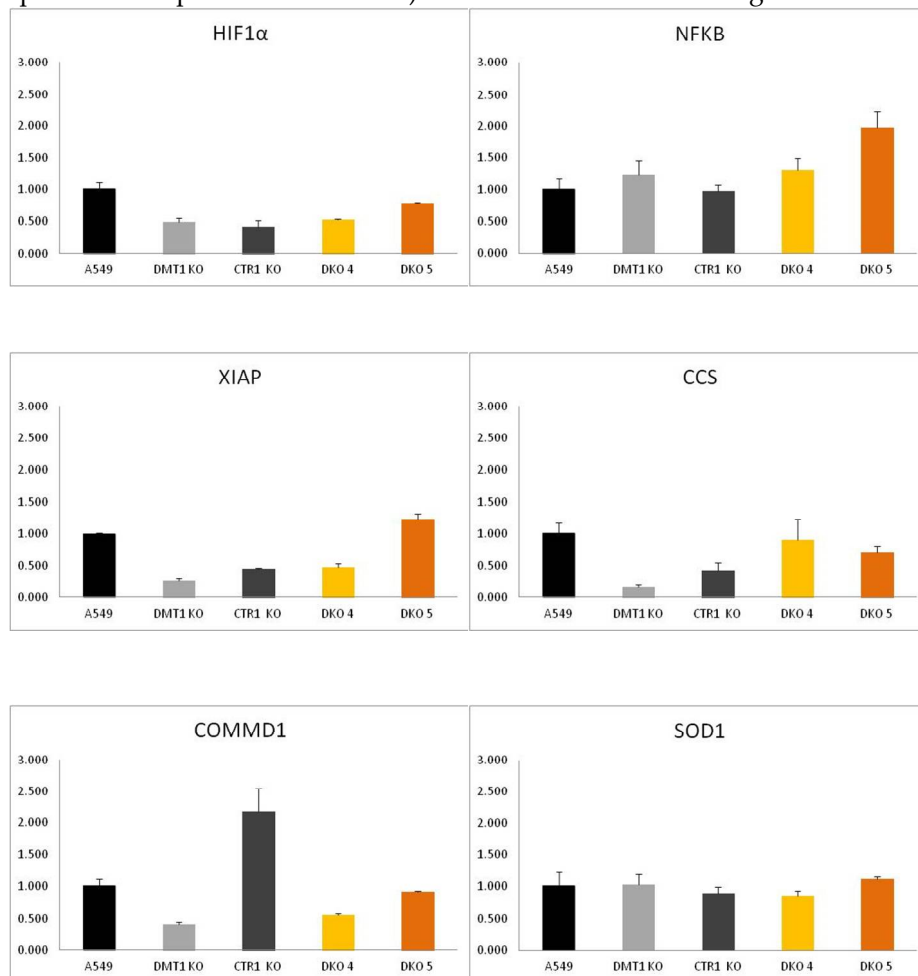
236

237

238

239

We next evaluated the pattern of gene expression for selected genes known to be linked to copper transport and more in general to copper homeostasis. In particular we tested at basal condition the expression of NF- $\kappa$ B (nuclear factor kappa-light-chain-enhancer of activated B cells), HIF1 $\alpha$  (hypoxia-inducible factor 1-alpha), SOD1 (Cu,Zn-superoxid dismutase), XIAP (X-linked inhibitor of apoptosis protein), COMMD1 (copper metabolism domain containing 1) and CCS (copper chaperone for superoxide dismutase). The results are shown in Figure 6.



240

241

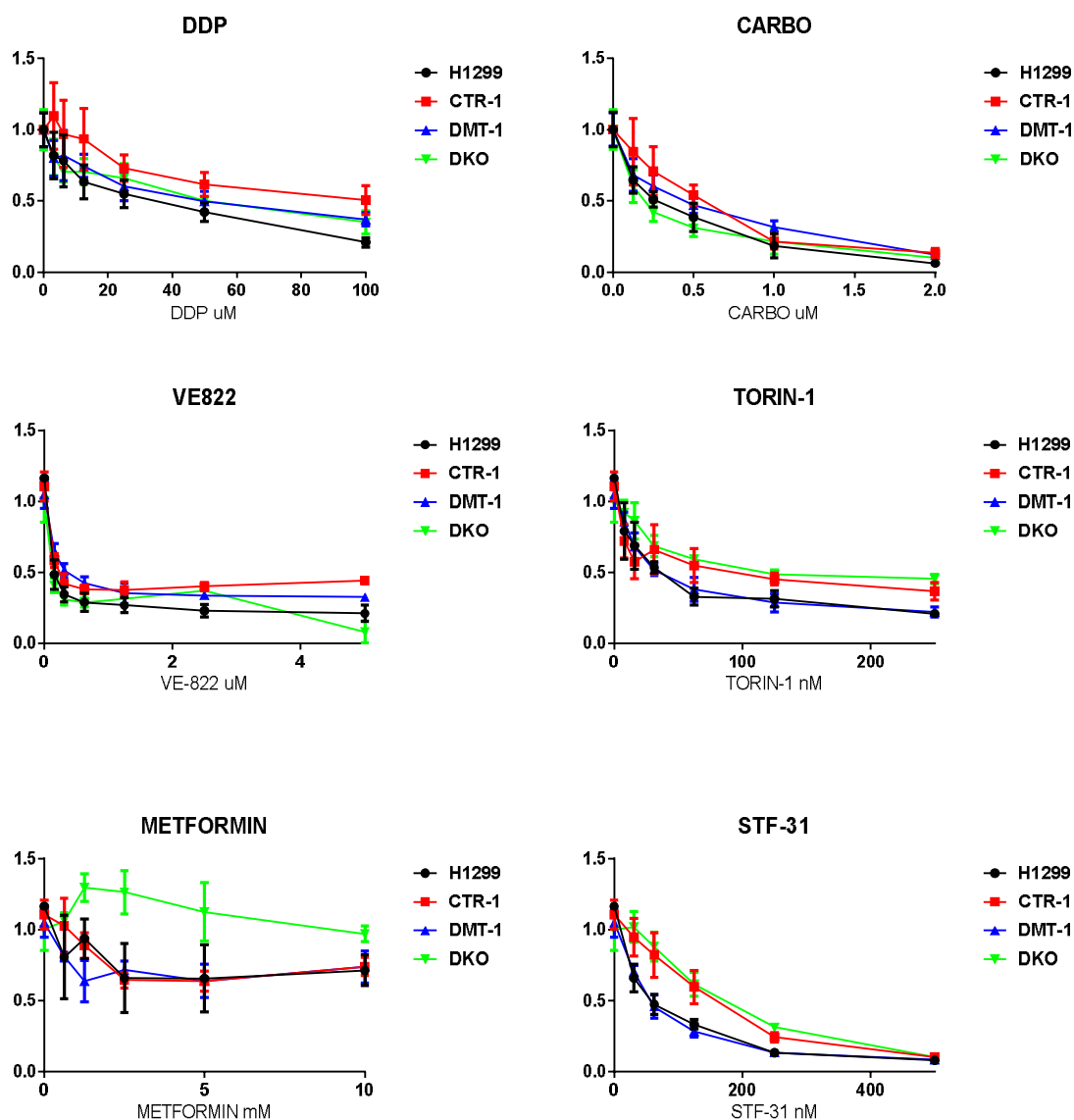
242

**Figure 6.** RT Real time expression PCR analysis of the mature mRNA concentration, which are the products genes related copper metabolism, in the different H1299-derived clones.

243 In DMT1-KO cells, the expression of the HIF1, COMMD1, XIAP, and CCS genes is reduced by  
 244 more than 2 times while NF- $\kappa$ B and SOD1 levels were almost unchanged. In CTR1-KO cells, a  
 245 decrease in HIF1, XIAP and CCS levels was also observed, but in contrast the expression of  
 246 COMMD1 gene was significantly increased, while NF- $\kappa$ B and SOD1 gene expression did not change  
 247 as in DMT-1 KO clones. DKO clones showed a mixed response, being HIF1 the only gene whose  
 248 expression was convincingly reduced. The expression of the other genes was either only slightly  
 249 decreased or remained unchanged.

250 Finally the clones were tested for their ability to respond to cytotoxic compounds, including  
 251 cisplatin (known substrates of CTR1 [11]), carboplatin (cisplatin analog), metformin, VE-822, Torin-1  
 252 and STF-31. The obtained results are presented in Figure 7.

253



254

255 **Figure 7.** Cytotoxic activity of cisplatin, carboplatin, VE-822, Torin-1, Metformin and STF-3 in H1299  
 256 parental cells and in KO derived. Absciss: drug concentrations,  $\mu$ M, Absciss: drug concentrations.  
 257 Ordinate: growth rate. Growth inhibitory activity was determined using the MTS test. Each point  
 258 represents the mean  $\pm$ SD of six replicates.

259 CTR1 KO cells were significantly more resistant to cisplatin than parental H1299 cells. The other  
 260 clones displayed cisplatin sensitivity similar to parental cells. Carboplatin showed similar activity in  
 261 parental and KO cells. VE-822, an inhibitor of the stress response ATR signaling pathway in DNA  
 262 repair [25]; TORIN-1, mTOR inhibitor, a member of phosphatidylinositol 3-kinase-related kinases



263 family, which functions as a serine/threonine protein kinase in different signaling way [26];  
264 displayed similar toxicity for all the clones. STF-31, specific glucose transporter 1 inhibitor [27],  
265 showed a slightly reduced activity in CTR-1 KO cells and even less in DKO clone. Meanwhile,  
266 interesting results were obtained with the AMPK inhibitor metformin, which decreases blood  
267 glucose concentration and is widely used in the treatment of obesity and now largely in some types  
268 of cancer [28]. With this drug parental cells and the single KO (both CTR-1 and DMT-1) behaved  
269 similarly. The both DKO clones were instead much less responsive.

#### 270 4. Discussion

271 The aim of this study was to generate and characterize the CTR1 and DMT1 single knockout  
272 and double CTR1/DMT1 knockout clones and to evaluate them as potential model for the studies of  
273 copper metabolism in catalytic and regulatory copper pools. The results will be mostly discussed  
274 with respect to the latter purpose. Doubling time of single KO clones derived from H1299 was  
275 similar to that of parent cells. Therefore, these cells are convenient for laboratory studies. As  
276 expected, only traces of CTR1-mRNA were detected in CTR1 KO/45 clone (Figure 1). Meanwhile,  
277 concentration of DMT1-mRNA increased by a factor of 1.6, generally agreeing with the observation  
278 that DMT1 can compensate the loss of CTR1 function and restore copper balance in the cell [16].  
279 However, in DMT1-KO clone the concentration of CTR1-mRNA did not change, thus suggesting  
280 that the compensation is gene-specific. In DKO clones, both CTR1 and DMT1 levels were almost  
281 absent, except for DMT-1 in DKO clone (heterozygous for DMT1) in which some DMT1 expression  
282 was detectable.

283 The loss of function of CTR1 or DMT1 genes in single KO clones led to copper deficiency in the  
284 cells and changed intracellular copper distribution (Figure 2). The copper levels in cytosol were  
285 strongly decreased as compared to parent line, but they were higher in CTR1 KO cells than in DMT1  
286 KO cells, again in line with the ability of DMT1 gene to compensate CTR1 function [16]. It also  
287 indicates that CTR1 gene cannot equally compensate loss of DMT1 function (Figure 1). It is likely  
288 that the decrease of copper levels in cytosol corresponds to the depletion of Cu-metallothionein [29].  
289 In mitochondria, copper concentrations did not significantly change as compared to parent line, in  
290 DMT1 KO cells its levels were even higher than in the wild type (Figure 2). It is possible that DMT1  
291 completely satisfies the copper requirements of mitochondria, maintaining the proper level of vitally  
292 important mitochondrial cytochrome-c-oxidase. In Golgi complex copper concentration decreased  
293 by a factor of 2 and 4 in CTR1 KO and DMT1 KO clones, respectively (Figure 2). In DKO5  
294 homozygous double knockout clone concentration of copper in all the isolated cellular fraction  
295 dropped below the used limit of detection. Copper could be detected only in mitochondria of  
296 DMT1-heterozygous clone DKO4.

297 We then used silver ions to compare the metal-transporting properties of CTR1 and DMT1 and  
298 to evaluate the difference between Cu(I) and Cu(II) transport routes. Cu(I) and Ag(I) have similar  
299 ion radii and the same structure of valence shells, so abiogenic Ag(I) is captured by Cu(I)-binding  
300 sites in CTR1 N-terminal domain and effectively transported into the cell. Accumulation of silver  
301 ions eventually leads to cell death [30]. Unlike CTR1, DMT1 does not contain thioether-rich  
302 metal-binding sites, so we supposed that CTR1-negative clones (CTR1 KO/45, CTR1 KO/46 and  
303 homozygous DKO5) would display increased resistance to silver ions as compared to wild type  
304 cells. Indeed, the cells that did not express CTR1 were more resistant to toxic effects of silver ions  
305 (Figure 3). Still DKO5 clone was the most resistant, indirectly proving that DMT1 can transfer both,  
306 Cu(II) and Cu(I)/Ag(I) [16].

307 The distribution of silver in the cells (Figure 4) of the parent line was in good agreement with  
308 known effects of Ag(I) binding by metallothionein [31], its accumulation in mitochondria [32] and its  
309 translocation to the lumen of Golgi complex [33]. We also paid attention that in the obtained clones,  
310 copper/silver is translocated to Golgi lumen (where secreted cuproenzymes are metallated) even in  
311 the conditions of copper deficiency. The loss of either CTR1 or DMT1 functions leads to the decrease  
312 in secretory ceruloplasmin synthesis and impairment of its metallation (apo-ceruloplasmin  
313 appeared in the secretion products) (Figure 5). It is established that the insertion of copper to

314 ceruloplasmin occurs in Golgi lumen and is catalyzed by copper-transporting P1 type ATPase  
315 (ATP7B). The copper is provided to ceruloplasmin by the following pathway: CTR1 → ATOX1 →  
316 ATP7B → ceruloplasmin [34]. Our present data indicate that copper atoms can be transported to  
317 Golgi lumen irrespectively from the import pathway.

318 The expression levels of genes, whose activity is linked or supposed to be linked to copper  
319 levels, were analyzed in the cells with the loss of CTR1 and/or DMT1 function. The results show that  
320 the genes under study were regulated differently (Figure 6). So SOD1 gene expression was not  
321 affected by CTR1 and/or DMT1 KO and was like that wild type cells.

322 Meanwhile, the activity of CCS gene coding Cu(I) chaperone for SOD1 decreased in single KO  
323 cells, but increased in DKO cells, in which copper cytosol concentration dropped below detection  
324 level. It is possible that in copper-deficient conditions apo-SOD1 is metallated in mitochondria [35],  
325 so the vital antioxidant function of holo-SOD1 is preserved. Thus, CCS gene may be activated when  
326 mitochondria use up all the copper that is not a part of cytochrome-c-oxidase pathway. However,  
327 the present data are insufficient to make reliable conclusions.

328 The decrease in expression of HIF1 $\alpha$  and XIAP genes occurred both in CTR1 and DMT1 single  
329 KO lines, but the cytosol copper deficiency, which was characteristic of DKO lines, may activate the  
330 expression if these genes, as well as the expression of NF- $\kappa$ B gene. It is possible that these genes were  
331 activated by indirect signals, rather than directly by copper deficiency.

332 The changes of COMMD1 expression levels observed in the different clones are the most  
333 interesting. COMMD1 expression was enhanced in CTR1-deficient cells and decreased in cells with  
334 DMT1-deficient cells. COMMD1 is currently the only member of intracellular copper metabolic  
335 system that is not an oxidoreductase, but binds copper in Cu(II) oxidation state [36]. COMMD1  
336 possesses sites for interaction with other copper transporters and may be viewed as a moonlighting  
337 protein [5]. Possibly, in wild type cells, COMMD1 received copper from DMT1 pathway, when  
338 DMT1 is knocked out and no copper is present in DMT1 pathway, COMMD1 gene expression  
339 decreases. In copper deficiency induced by the loss of CTR1 function, the role of COMMD1 in  
340 copper metabolism increases. Even if this is an attractive hypothesis, does not completely explain the  
341 levels of COMMD1-mRNA in DKO clones, which are similar to the levels present in the wild type  
342 cells. This could be the result of the sum of the effects of DMT1 KO (inducing a decrease of  
343 COMMD1 mRNA levels) and CTR1 (which instead increases COMMD1 expression) although this  
344 remains at present a speculation.

345 Tests for sensitivity of the obtained cells to various drugs (Figure 7) proved the fact, that the loss  
346 of CTR1, but not DMT1 rendered the cells resistant to cisplatin [12]. Other drugs, which were tested  
347 in the present work, affected the viability of the CTR1 KO, DMT1 KO, DKO and WT cells in similar  
348 manner. The only clear exception was metformin: DKO5 cells displayed resistance when exposed to  
349 this drug. Metformin has very diverse spectrum of interactions [28], including the ability to bind and  
350 transfer copper atoms [37], the latter may enhance the viability of copper deficient DKO5 cells. Being  
351 metformin widely used for different indication, including cancer, the knowledge that copper levels  
352 or transport can modify its activity could have, if confirmed important implications.

353 In summary the results obtained in the present work represents a good evidence that isogenic  
354 cell lines with differential knockouts of copper transporters and discriminated copper import  
355 pathways will be useful for studies of regulatory role of copper and could also have important  
356 translational relevance.

357 **Author Contributions:** Conceptualization: M.B., L.V.P.; First draft of the manuscript: M.B., L.V.P., E.Y.I.,  
358 Investigation: E.Y.I., E.B., I.A.O., E.A.S., M.B., L.V.P.; Resources: M.B., L.V.P., E.Y.I.; Figures: M.B., E.Y.I.,  
359 L.V.P.; Co-author of conceptualization and critical revision of the manuscript for important intellectual  
360 content: E.Y.I., I.A.O.

361 **Funding:** The work was supported by grants: RFBR 16-34-60219, 18-015-00481, MK2718.2018.4.

362 **Conflicts of Interest:** The authors declare no conflict of interest. The funders had no role in the design of the  
363 study; in the collection, analyses, or interpretation of data; in the writing of the manuscript, or in the decision to  
364 publish the results.

365 **References**

- 366 1. Vonk, W.I.; Wijmenga, C.; van de Sluis, B. Relevance of animal models for understanding mammalian  
367 copper homeostasis. *Am. J. Clin. Nutr.* **2008**, *88*, 840S–5S. doi:10.1093/ajcn/88.3.840S.
- 368 2. Ridge, P.G.; Zhang, Y.; Gladyshev, V.N. Comparative genomic analyses of copper transporters and  
369 cuproproteomes reveal evolutionary dynamics of copper utilization and its link to oxygen. *PLoS ONE*  
370 **2008**, *3*, e1378. doi:10.1371/journal.pone.0001378.
- 371 3. Li, S.; Zhang, J.; Yang, H.; Wu, C.; Dang, X.; Liu, Y. Copper depletion inhibits CoCl<sub>2</sub>-induced aggressive  
372 phenotype of MCF-7 cells via downregulation of HIF-1 and inhibition of Snail/Twist-mediated  
373 epithelial-mesenchymal transition. *Sci. Rep.* **2015**, *5*, 12410. doi:10.1038/srep12410.
- 374 4. Hou, M.M.; Polykretis, P.; Luchinat, E.; Wang, X.; Chen, S.N.; Zuo, H.H.; et al. Solution structure and  
375 interaction with copper in vitro and in living cells of the first BIR domain of XIAP. *Sci. Rep.* **2017**, *7*, 16630.  
376 doi:10.1038/s41598-017-16723-5.
- 377 5. Riera-Romo, M. COMMD1: A multifunctional regulatory protein. *J. Cell. Biochem.* **2018**, *119*, 34–51.  
378 doi:10.1002/jcb.26151.
- 379 6. Bartuzi, P.; Hofker, M.H.; van de Sluis, B. Tuning NF-κB activity: a touch of COMMD proteins. *Biochim.*  
380 *Biophys. Acta.* **2013**, *1832*, 2315–2321. doi: 10.1016/j.bbadis.2013.09.014.
- 381 7. Ostrakhovitch, E.A.; Song, Y.P.; Cherian, M.G. Basal and copper-induced expression of metallothionein  
382 isoform 1,2 and 3 genes in epithelial cancer cells: The role of tumor suppressor p53. *J. Trace Elem. Med. Biol.*  
383 **2016**, *35*:18–29. doi:10.1016/j.jtemb.2016.01.008.
- 384 8. Bhattacharjee, A.; Chakraborty, K.; Shukla, A. Cellular copper homeostasis: current concepts on its  
385 interplay with glutathione homeostasis and its implication in physiology and human diseases. *Metallomics*  
386 **2017**, *9*, 1376–1388. doi:10.1039/c7mt00066a.
- 387 9. Kardos, J.; Héja, L.; Simon, Á.; Jablonkai, I.; Kovács, R.; Jemnitz, K. Copper signalling: causes and  
388 consequences. *Cell Commun. Signal.* **2018**, *16*, 71. doi:10.1186/s12964-018-0277-3.
- 389 10. Sharp, P.A. Ctr1 and its role in body copper homeostasis. *Int. J. Biochem. Cell. Biol.* **2003**, *35*, 288–291.  
390 doi:10.1016/S1357-2725(02)00134-6.
- 391 11. Kilari, D.; Guancial, E.; Kim, E.S. Role of copper transporters in platinum resistance. *World J. Clin. Oncol.*  
392 **2016**, *7*, 106–113. doi:10.5306/wjco.v7.i1.106.
- 393 12. Lasorsa, A.; Natile, G.; Rosato, A.; Tadini-Buoninsegni, F.; Arnesano, F. Monitoring interactions inside  
394 cells by advanced spectroscopies: Overview of copper transporters and cisplatin. *Curr. Med. Chem.* **2018**, *25*,  
395 462–477. doi:10.2174/0929867324666171110141311.
- 396 13. Gunshin H., Mackenzie, B.; Berger, U.V.; Gunshin, Y.; Romero, M.F.; Boron, W.F. et al. Cloning and  
397 characterization of a mammalian proton-coupled metal-ion transporter, *Nature.* **1997**, *388*, 482–488. doi:  
398 10.1038/41343
- 399 14. Czachorowski, M.; Lam-Yuk-Tseung, S.; Cellier, M.; Gros, P. Transmembrane topology of the mammalian  
400 Slc11a2 iron transporter. *Biochemistry.* **2009**, *48*, 8422–8434. doi: 10.1021/bi900606y.
- 401 15. Wang, D.; Song, Y.; Li, J.; Wang, C.; Li, F. Structure and metal ion binding of the first transmembrane  
402 domain of DMT1. *Biochim. Biophys. Acta.* **2011**, *1808*, 1639–1644. doi:10.1016/j.bbamem.2010.11.005.
- 403 16. Arredondo, M.; Munoz, P.; Mura, C.V.; Nunez, M.T. DMT1, a physiologically relevant apical Cu<sup>1+</sup>  
404 transporter of intestinal cells. *Am. J. Physiol. Cell. Physiol.* **2003**, *284*, C1525–C1530.  
405 doi:10.1152/ajpcell.00480.2002.
- 406 17. Lin, C.; Zhang, Z.; Wang, T.; Chen, C.; Kang, Y.J. Copper uptake by DMT1: A compensatory mechanism  
407 for CTR1 deficiency in human umbilical vein endothelial cells. *Metallomics* **2015**, *7*, 1285–1289.  
408 doi:10.1039/c5mt00097a.
- 409 18. Zatulovskaia, Y.A.; Ilyechova, E.Y.; Puchkova, L.V. The features of copper metabolism in the rat liver  
410 during development. *PLoS ONE* **2015**, *10*, e0140797. doi:10.1371/journal.pone.0140797.
- 411 19. Samygina, V.R.; Sokolov, A.V.; Bourenkov, G.; Schneider, T.R.; Anashkin, V.A.; Kozlov, S.O.; et al. Rat  
412 ceruloplasmin: A new labile copper binding site and zinc/copper mosaic. *Metallomics* **2017**, *9*, 1828–1838.  
413 doi:10.1039/c7mt00157f.
- 414 20. Bielli, P.; Calabrese, L. Structure to function relationships in ceruloplasmin: A ‘moonlighting’ protein. *Cell.*  
415 *Mol. Life Sci.* **2002**, *59*, 1413–1427. doi:10.1007/s00018-002-8519-2.
- 416 21. Golenkina, E.A.; Viryasova, G.M.; Galkina, S.I.; Gaponova, T.V.; Sud’ina, G.F.; Sokolov, A.V. Fine  
417 regulation of neutrophil oxidative status and apoptosis by ceruloplasmin and its derivatives. *Cells* **2018**, *7*,  
418 E8. doi:10.3390/cells7010008.

- 419 22. Bernevic, B.; El-Khatib, A.H.; Jakubowski, N.; Weller, M.G. Online immunocapture ICP-MS for the  
420 determination of the metalloprotein ceruloplasmin in human serum. *BMC Res. Notes* **2018**, *11*, 213.  
421 doi:10.1186/s13104-018-3324-7.
- 422 23. Fleming, R.E.; Whitman, I.P.; Gitlin, J.D. Induction of ceruloplasmin gene expression in rat lung during  
423 inflammation and hyperoxia. *Am J Physiol.* **1991**, *260*, L68-74. doi: 10.1152/ajplung.1991.260.2.L68
- 424 24. Babich, P.S.; Skvortsov, A.N.; Rusconi, P.; Tsymbalenko, N.V.; Mutanen, M.; Puchkova, L.V.; Broggin, M.  
425 Non-hepatic tumors change the activity of genes encoding copper trafficking proteins in the liver. *Cancer*  
426 *Biol Ther.* **2013**, *14*, 614-624. doi:10.4161/cbt.24594
- 427 25. Rahal, O.N.; Fatfat, M.; Hankache, C.; Osman, B.; Khalife, H.; Machaca, K.; Muhtasib, H.G. Chk1 and  
428 DNA-PK mediate TPEN-induced DNA damage in a ROS dependent manner in human colon cancer cells.  
429 *Cancer Biol. Ther.* **2016**, *17*, 1139-1148. doi:10.1080/15384047.2016.1235658
- 430 26. Hare, S.H.; Harvey, A.J. mTOR function and therapeutic targeting in breast cancer. *Am. J. Cancer Res.* **2017**,  
431 *7*, 383-404.
- 432 27. Chan, D.A.; Sutphin, P.D.; Nguyen, P.; Turcotte, S.; Lai, E.W.; Banh, A.; et al. Targeting GLUT1 and the  
433 Warburg effect in renal cell carcinoma by chemical synthetic lethality. *Sci. Transl. Med.* **2011**, *3*, 94ra70.  
434 doi:10.1126/scitranslmed.3002394.
- 435 28. Schulten, H.J. Pleiotropic effects of metformin on cancer. *Int. J. Mol. Sci.* **2018**, *19*, pii: E2850.  
436 doi:10.3390/ijms19102850.
- 437 29. Calvo, J.; Jung, H.; Meloni, G. Copper metallothioneins. *IUBMB Life.* **2017**, *69*, 236-245.  
438 doi:10.1002/iub.1618.
- 439 30. Bertinato, J.; Cheung, L.; Hoque, R.; Plouffe, L.J. Ctr1 transports silver into mammalian cells. *J. Trace Elem.*  
440 *Med. Biol.* **2010**, *24*, 178-184. doi:10.1016/j.jtemb.2010.01.009.
- 441 31. Palacios, O.; Polec-Pawlak, K.; Lobinski, R.; Capdevila, M.; González-Duarte, P. Is Ag(I) an adequate probe  
442 for Cu(I) in structural copper-metallothionein studies? The binding features of Ag(I) to mammalian  
443 metallothionein 1. *J. Biol. Inorg. Chem.* **2003**, *8*, 831-842. doi:10.1007/s00775-003-0481-4.
- 444 32. Zatulovskiy, E.A.; Skvortsov, A.N.; Rusconi, P.; Ilyechova, E.Y.; Babich, P.S.; Tsymbalenko, N.V.; Broggin,  
445 M.; Puchkova, L.V. Serum depletion of holo-ceruloplasmin induced by silver ions in vivo reduces utake of  
446 cisplatin. *J. Inorg. Biochem.* **2012**, *116*, 88-96. doi:10.1016/j.jinorgbio.2012.07.003.
- 447 33. Ilyechova, E.Y.; Saveliev, A.N.; Skvortsov, A.N.; Babich, P.S.; Zatulovskaia, Y.A.; Pliss, M.G.; et al. The  
448 effects of silver ions on copper metabolism in rats. *Metallomics* **2014**, *6*, 1970-1987. doi:10.1039/c4mt00107a
- 449 34. Polishchuk, R.; Lutsenko, S. Golgi in copper homeostasis: a view from the membrane trafficking field.  
450 *Histochem. Cell Biol.* **2013**, *140*, 285-295. doi:10.1007/s00418-013-1123-8.
- 451 35. Baker, Z.N.; Cobine, P.A.; Leary, S.C. The mitochondrion: a central architect of copper homeostasis.  
452 *Metallomics* **2017**, *15*, 9, 1501-1512. doi:10.1039/c7mt00221a.
- 453 36. Narindrasorasak, S.; Kulkarni, P.; Deschamps, P.; She, Y.M.; Sarkar, B. Characterization and copper  
454 binding properties of human COMMD1 (MURR1). *Biochemistry* **2007**, *46*, 3116-3128. doi:10.1021/bi0620656.
- 455 37. Logie, L.; Harthill, J.; Patel, K.; Bacon, S.; Hamilton, D.L.; Macrae, K.; et al. Cellular responses to the  
456 metal-binding properties of metformin. *Diabetes* **2012**, *61*, 1423-1433. doi:10.2337/db11-0961.